Journal of Cranio-Maxillo-Facial Surgery 47 (2019) 1589–1599

Contents lists available at ScienceDirect

Journal of Cranio-Maxillo-Facial Surgery

journal homepage: www.jcmfs.com

Targeting inhibitors of apoptosis in oral squamous cell carcinoma *in vitro*

Mario J.J. Scheurer [a, *], Axel Seher [a], Valentin Steinacker [a], Christian Linz [a], Stefan Hartmann [a, b], Alexander C. Kübler [a], Urs D.A. Müller-Richter [a], Roman C. Brands [a, c]

[a] Department of Oral and Maxillofacial Plastic Surgery (Head: A. C. Kübler), University Hospital Würzburg, Pleicherwall 2, 97070 Würzburg, Germany
[b] Interdisciplinary Center for Clinical Research (Head: M. Goebeler), University Hospital Würzburg, Josef-Schneider-Str. 2, 97080 Würzburg, Germany
[c] Comprehensive Cancer Center Mainfranken (CCC MF) (Head: R. C. Bargou), Josef-Schneider-Str. 6, 97080 Würzburg, Germany

ARTICLE INFO

Article history:
Paper received 16 January 2019
Accepted 14 July 2019
Available online 19 July 2019

Keywords:
LCL161
Oral squamous cell carcinoma
Inhibitor of apoptosis proteins
SMAC mimetics
FasL
Apoptosis

ABSTRACT

Head and neck cancer, which predominantly arises from the oral mucosa, represents the sixth most common malignancy worldwide. These cancer cells can be resistant to programmed cell death triggered by extrinsic stimuli due to innate overexpression of inhibitor of apoptosis proteins (IAPs). The cellular protein second mitochondria-derived activator of caspases (SMAC) can antagonize IAP-induced caspase inhibition and thus trigger apoptosis. Here, we investigate the cell death-sensitizing effects of the SMAC mimetic LCL161 alone and in combination with Fas ligand (FasL) using a panel of six cell lines. Fas receptor (FasR) expression was analyzed by flow cytometry. Cells were treated with FasL and LCL161 alone or in combination, and cytotoxicity was measured using crystal violet assays. Annexin V and cell viability assays using zVAD-fmk and Necrostatin-1 (Nec-1) were carried out to assess the type of programmed cell death induced by LCL161. To demonstrate the sensitizing effects of LCL161, we employed the t-test to compare the effects of FasL alone and in combination with LCL161. Linear regression analysis was performed to determine initial and half maximal inhibitory concentrations (IC_{10} and IC_{50}, respectively). Distinct FasR expression was detected in each cell line. Four of six cell lines were significantly sensitized to FasL by LCL161 ($p < 0.05$), and synergistic effects were observed ($y < 1$). Moreover, the initially resistant cell line SCC-25 was effectively sensitized to FasL by LCL161. Annexin V FACS analysis demonstrated apoptosis-sensitizing and apoptosis-inducing effects of LCL161 across all cell lines. Using specific cell death inhibitors (zVAD-fmk and Nec-1), we demonstrated that LCL161-initiated apoptosis could not be prevented, highlighting the proapoptotic potential of this mimetic in these cells. Our findings show the effectiveness of apoptotic sensitization of OSCC cells by LCL161 in combination with FasL, thus confirming the importance of an IAP-targeting therapeutic approach for oral squamous cell carcinoma.

1. Introduction

Carcinomas of the head and neck, 40% of which consists of oral squamous cell carcinoma (OSCC), are the sixth most common malignant neoplasias worldwide, with approximately 600,000 and 300,000 new cases and deaths per year, respectively (Jou and Hess, 2017; Döbrossy, 2005). In most cases, head and neck cancer constitutes squamous cell carcinoma, which originates from the mucosal site of the oral cavity (Vigneswaran and Williams, 2014). Multimodal treatment procedures consisting of surgery, radiotherapy and chemotherapy still result in five-year survival rates between 50 and 60%, a poor prognosis (Gupta et al., 2009). Recent therapeutic strategies for OSCC also include immunotherapy and targeted therapy, which are mostly directed toward overexpression of epidermal growth factor receptor (EGFR) (Grandis and Tweardy, 1993). However, therapeutic antibodies such as cetuximab and panitumumab exhibit low treatment efficacy and are accompanied by serious adverse effects (Matta and Ralhan, 2009). Other agents, such as tyrosine kinase inhibitors (TKIs), which also target EGFR, reportedly have no significant impact on OSCC in clinical trials (Chapman et al., 2016). Nonetheless, the recently approved agents nivolumab and pembrolizumab

* Corresponding author. Department of Oral and Maxillofacial Plastic Surgery, University Hospital Würzburg, Pleicherwall 2, 97070 Würzburg, Germany.
E-mail address: MarioScheurer@icloud.com (M.J.J. Scheurer).

https://doi.org/10.1016/j.jcms.2019.07.022
1010-5182/

demonstrate promising potential due to their ability to modulate the behavior of T cells and help them overcome immunosuppressive signals from the tumor microenvironment (TME) (Ribas, 2012). Therefore, new pathways of targeted molecular therapies should be analyzed. Recent therapeutic strategies include inducing programmed cell death, such as apoptosis, in cancer cells. Apoptosis can be activated by extrinsic or intrinsic pathways. Receptors such as Fas receptor (FasR) activate extrinsic apoptosis in response to external stimuli, as mediated by cytokines originating from the TME, including tumor necrosis factor α (TNF-α) and Fas ligand (FasL) (Nikoletopoulou et al., 2013). The binding of FasL to FasR leads to trimerization of the receptor and formation of the death-inducing signaling complex (DISC), which initiates a caspase cascade that results in cellular degradation (Elmore, 2007). Oxidative or genotoxic stress activates the intrinsic apoptotic pathway; permeabilized by proteins of the B-cell lymphoma 2 (Bcl-2) family, mitochondria release second mitochondria-derived activator of caspases (SMAC), forming the apoptosome. This complex promotes caspase activation, which results in intrinsic apoptosis (Du et al., 2000).

Upregulation of antiapoptotic proteins is a strategy by which OSCC cells circumvent cell death, which describes one of Hanahan and Weinberg's "Hallmarks of Cancer" (Hanahan and Weinberg, 2011). These molecules identified by Crook et al. (1993) are termed inhibitors of apoptosis (IAP) proteins and contain characteristic baculovirus IAP repeat (BIR) domains for caspase binding and inhibition (Deveraux and Reed, 1999). Overexpression of cellular IAP (cIAP)-1, cIAP2 and X-linked IAP (XIAP) is correlated with OSCC occurrence and lymph node metastasis (Qi et al., 2008; Nagata et al., 2011; Tamatani et al., 2012; Tanimoto et al., 2005). Hence, these proteins play an important role in cancer development and are responsible for therapy resistance and poor prognosis (LaCasse et al., 2008). Retrospective analysis of data from the Cancer Genome Atlas (TCGA) indicates that these alterations influence overall survival (Gao et al., 2013; Cerami et al., 2012). In addition to blocking programmed cell death, IAPs regulate nuclear factor kappa-light-chain-enhancer of activated B-cells (NF-κB), leading to inflammation, immune responses, migration and survival (Gyrd-Hansen and Meier, 2010). As a direct IAP antagonist, the protein SMAC induces caspase-driven apoptosis. By mimicking the IAP-binding motif, SMAC mimetics act as potent agents for IAP inhibition or degradation in OSCC (Bai et al., 2014), stimulating IAP E3 ubiquitin ligase activity and thus directing these proteins toward proteasomal degradation (Fulda, 2015).

This study aimed to detect the therapeutic effects of the SMAC mimetic compound LCL161 alone and in combination with FasL, and the results illustrate the potential proapoptotic sensitization of OSCC cells *in vitro*.

2. Materials and methods

2.1. Cell culture

OSCC cell lines were purchased from ATCC (LGC Standards, Wesel, Germany) and maintained in specific culture media (Table 1) supplemented with 10% fetal calf serum (FCS; Thermo Fisher Scientific, Darmstadt, Germany) and 1% penicillin/streptomycin (P/S; Thermo Fisher Scientific). The culture conditions were 5% CO_2 and a 37 °C humidified atmosphere. Cell passaging was performed every 72 h using PBS (Thermo Fisher Scientific) to eliminate dead cells from the culture. Adherent cells were detached using 0.25% (w/v) trypsin/0.53 mM EDTA solution (Biochrom, Berlin, Germany). Cell numbers were determined using a CASY cell counter and analyzer model TT (Schärfe System, Reutlingen, Germany).

2.2. Agents and ligands

LCL161 (Novartis, Basel, Switzerland) was purchased from Selleck Chemicals Europe (Absource Diagnostics, Munich, Germany) and stored in accordance with the manufacturer's instructions in dimethyl sulfoxide (DMSO) at −20 °C. Human Fc-FLAG-FasL was isolated from stably transfected HEK293 cells. Secreted FLAG-tagged soluble FasL was purified from supernatants by affinity chromatography using anti-FLAG M2 agarose beads (Sigma−Aldrich, Schnelldorf, Germany) (Brands et al., 2018; Lagler et al., 2017).

2.3. Cytotoxicity assay

Cells were seeded in triplicate at 1×10^4 cells/well in 100 µl medium in 96-well plates (Thermo Fisher Scientific). After reattachment overnight, the cells were stimulated with LCL161 as a single agent in log2 dilutions for 72 h. A similar procedure was performed for FasL incubation. For dual agent treatment, constant IC_{10} doses of LCL161 were combined with log2 dilutions of FasL. Selected concentrations were adopted from the literature (Yang et al., 2016; Brands et al., 2016). At the appropriate time points, the culture medium was removed and replaced with 50 µl crystal violet solution (0.5 g crystal violet [Carl Roth, Karlsruhe, Germany], 100 ml methanol [Sigma−Aldrich] and 400 ml dH_2O) for 12 min, and the plates were washed with dH_2O and dried overnight. After dissolving in 100 µl methanol/well, absorbance was measured at 595 nm using a Tecan Infinite F50 absorbance microplate reader (Tecan Group, Männedorf, Switzerland). Mean values were calculated from three independently executed experiments.

2.4. FACS analyses of FasR and Annexin V/7-AAD

FasR (resp. CD95) analysis was performed using PE-conjugated mouse anti-human CD95 monoclonal antibody (BD Biosciences, Heidelberg, Germany), as previously described (Brands et al., 2018).

To demonstrate apoptosis induction by LCL161, we performed Annexin V PE and 7-AAD dual-color FACS analysis using an eBioscience Annexin V Apoptosis Detection Kit PE (Thermo Fisher Scientific). Flow cytometry was carried out with BD FACSCalibur and BD CellQuest Pro version 5.1 software (BD Biosciences). FlowJo version 10 (FlowJo LLC, Ashland, USA) was used for data analysis and graph plotting. To subdivide the dot plots into quadrants (Q1 to

Table 1
OSCC cell lines. Information on the cell lines, characteristics and specific culture medium including supplements of cells used in this study. Non-OSCC cell lines A-253 and HaCaT are marked by asterisks and included in this panel as references.

Cell lines	Collection sites & characteristics	Culture media + supplements
Detroit 562	Metastatic site of pharyngeal carcinoma from female caucasian patient	MEM Alpha + 10% FCS + 1% P/S
FaDu	Primary hypopharyngeal carcinoma from male caucasian patient	MEM Alpha + 10% FCS + 1% P/S
SCC-9	Primary tongue carcinoma from 25 years male patient	DMEM/F-12 (1:1) + 10% FCS + 1% P/S + 5 µ1 hydrocortisone
SCC-25	Primary tongue carcinoma from 70 years male patient	DMEM/F-12 (1:1) + 10% FCS + 1% P/S + 5 µ1 hydrocortisone
A-253*	Epidermoid carcinoma of submaxillary salivary gland from 54 years male caucasian patient	McCoy's 5A + 10% FCS + 1% P/S
HaCaT*	Immortalised human keratinocytes	DMEM + 10% FCS + 1% P/S

Q4), we placed quadrant markers based on preliminary investigations using untreated control HaCaT cells, for which the bulk of the cell population was located at Q4 (data not shown). Q1 (Annexin V−/7-AAD+) shows nonspecific cell death. Q2 (Annexin V+/7-AAD+) corresponds to the late stage of apoptosis. In contrast, Q3 (Annexin V+/7-AAD−) indicates early apoptosis because of the lack of 7-AAD staining resulting from intact cell membranes. Living cells are located in Q4 (Annexin V−/7-AAD−).

2.5. Cell viability assay

Viability detection of OSCC cells stimulated by LCL161 was conducted using crystal violet cytotoxicity assays. A sample of approximately 1×10^4 cells was seeded in 100 μl medium in 96-well plates and incubated overnight. After reattachment, the cells were treated with the approximate maximum inhibitory concentration of LCL161 (IC_{90}; Table 2), the pan-caspase inhibitor benzyloxycarbonyl-Val-Ala-Asp (OMe) fluoromethylketone (zVAD-fmk; 50 μM; Bachem, Weil am Rhein, Germany), the necroptosis inhibitor Necrostatin-1 (Nec-1; 90 μM; Enzo Life Sciences, Lörrach, Germany) or a combination of these agents for 24 h. The biological activity of zVAD-fmk and Nec-1 has been described by Lagler et al. (2017). Cell quantification was performed by measuring absorbance at 595 nm using a microplate reader (Tecan Group).

2.6. Statistical analysis

Data were analyzed with Microsoft Excel 2016 (Microsoft Corporation, Redmond, USA), GraphPad Prism (version 6.04; GraphPad Software, La Jolla, USA) and MEDAS (Grund EDV-Systeme, Margetshöchheim, Germany). Student's t-test was used to compare FasL alone with FasL and LCL161 in combination; p-values <0.05 indicated statistically significant effects of the combination and supported the hypothesis that LCL161 sensitizes OSCC cells to FasL. The inhibitory concentration of LCL161 that reduced relative cell numbers by 10% was termed IC_{10}. To contrast the impact of FasL alone with the FasL and LCL161 combination, we calculated half maximal inhibitory concentrations (IC_{50}) via linear regression analysis. Quantitative therapy assessment was conducted using Tallarida's interaction index y (Tallarida, 2002), whereby $y < 1$ was considered to indicate synergistic effects of the combination therapy and $y > 1$ was considered to indicate antagonistic effects.

3. Results

3.1. FasR expression in OSCC

To test whether the resistance of OSCC cells to FasL arises from the absence of FasR, we performed flow cytometry analysis of FasR expression. All OSCC cell lines demonstrated distinct levels of FasR expression represented by the percentage of FasR+ cells relative to that in the control group (Fig. 1).

Table 2
Inhibitory doses of the SMAC mimetic compound LCL161 in OSCC cells (μM). LCL161 concentrations were individually determined for each cell line. For this purpose, at least three independent experiments were carried out to calculate the average value ($n = 3$).

Cell lines	LCL161			
	IC_{10}	IC_{50}	IC_{90}	IC_{100}
Detroit 562	18.8	48.7	97.7	200
FaDu	25	61.2	91.7	100
SCC-9	1.1	21.6	100	200
SCC-25	0.9	19.8	125	200
A-253	23.9	64.3	95.8	100
HaCaT	0.6	29.1	79.2	100
Cumulative	**14.2**	**40.8**	**98.2**	**150**

3.2. Dose-dependent efficacy of LCL161 alone

Based on the heterogeneous responsiveness of OSCC cells towards FasL (Brands et al., 2018), we assessed whether intrinsic IAPs might be responsible for therapeutic resistance using cytotoxicity assays performed with log2 dilutions of LCL161 (Fig. 2). The entire cell panel showed a dose-dependent reduction in cell count in response to LCL161 treatment. For Detroit 562 and FaDu cells, a decrease in the relative cell number was observed at LCL161 concentrations >12.5 μM. In contrast, less than half the dose of LCL161 induced half maximal inhibition in SCC-9 and SCC-25 cells (Table 2). The obtained IC_{50} values of LCL161 ranging from 19.8 to 64.3 μM are in accordance with previously published data (Yang et al., 2015; Ramakrishnan et al., 2014). This analysis was the basis for calculating the initial inhibitory concentration (IC_{10}) for the combination of LCL161 with FasL. The minimal inhibitory dose was 18.8 μM for Detroit 562 cells, 25 μM for FaDu cells, 1.1 μM for SCC-9 cells and 0.9 μM for SCC-25 cells. The IC_{10} values for the reference cell lines A-253 and HaCaT were 23.9 μM and 0.6 μM, respectively.

3.3. Effects of FasL on OSCC cells

Overall, heterogeneous susceptibility toward FasL was observed, with a subdivision of the cell panel into two groups (Fig. 3). Three of the six cell lines (Detroit 562, FaDu and HaCaT) exhibited a dose-dependent response to FasL. The highest efficacy of FasL was found in Detroit 562 cells, whereby a FasL concentration of 200 ng/ml reduced the relative cell count to 29.8% (±6.1%), with an IC_{50} of 51.1 ng/ml. The maximum achievable decrease in relative cell count for FaDu cells was 62.8% (±9.5%) at 200 ng/ml FasL (IC_{50}: not definable). In control HaCaT cells, FasL [200 ng/ml] reduced proliferation to 52% (±11.2%), with an IC_{50} of 51.2 ng/ml. In contrast, FasL [200 ng/ml] induced no decline in cell vitality (IC_{50}: not definable) in the remaining cell lines (SCC-9, SCC-25 and A-253); thus, we classified these cells as nonresponsive to FasL.

3.4. LCL161 sensitizes OSCC cells to FasL

Cells were incubated for 72 h at the IC_{10} concentration of LCL161 in combination with log2 dilutions of FasL (Fig. 3). Four of the six cell lines (Detroit 562, FaDu, SCC-25 and HaCaT) showed significant responses to this combination. The FasL-responsive cell lines Detroit 562 and FaDu displayed synergistic effects in response to LCL161 + FasL ($y < 1$) (Table 3), and in both cell lines, LCL161 (at IC_{10}) potentiated the cytotoxicity of FasL by more than 30 times. Comparing the combination with FasL alone, Detroit 562 and FaDu cells displayed significant ($p < 0.05$) to very highly significant ($p < 0.001$) sensitization effects. Of note, LCL161 (IC_{10} of 0.9 μM) sensitized the previously nonresponsive cell line SCC-25 to FasL, demonstrating synergistic effects ($y < 1$). Highly ($p < 0.01$) to very highly significant effects ($p < 0.001$) of the combination were also observed at FasL doses ranging from 1.56 to 200 ng/ml. However, in FasL-resistant SCC-9 cells, no cytotoxic effects were observed in response to the combination of LCL161 and FasL ($p > 0.35$). According to Tallarida's interaction index, antagonistic effects were validated for this cell line. The FasL-resistant reference cell line A-253 behaved in a similar manner ($p > 0.14$; $y > 1$), with no cytotoxicity mediated by LCL161 (IC_{10} of 23.9 μM), and HaCaT cells demonstrated moderate responsiveness to FasL monotherapy. In comparison, LCL161 (IC_{10} of 0.6 μM) had distinct synergistic effects

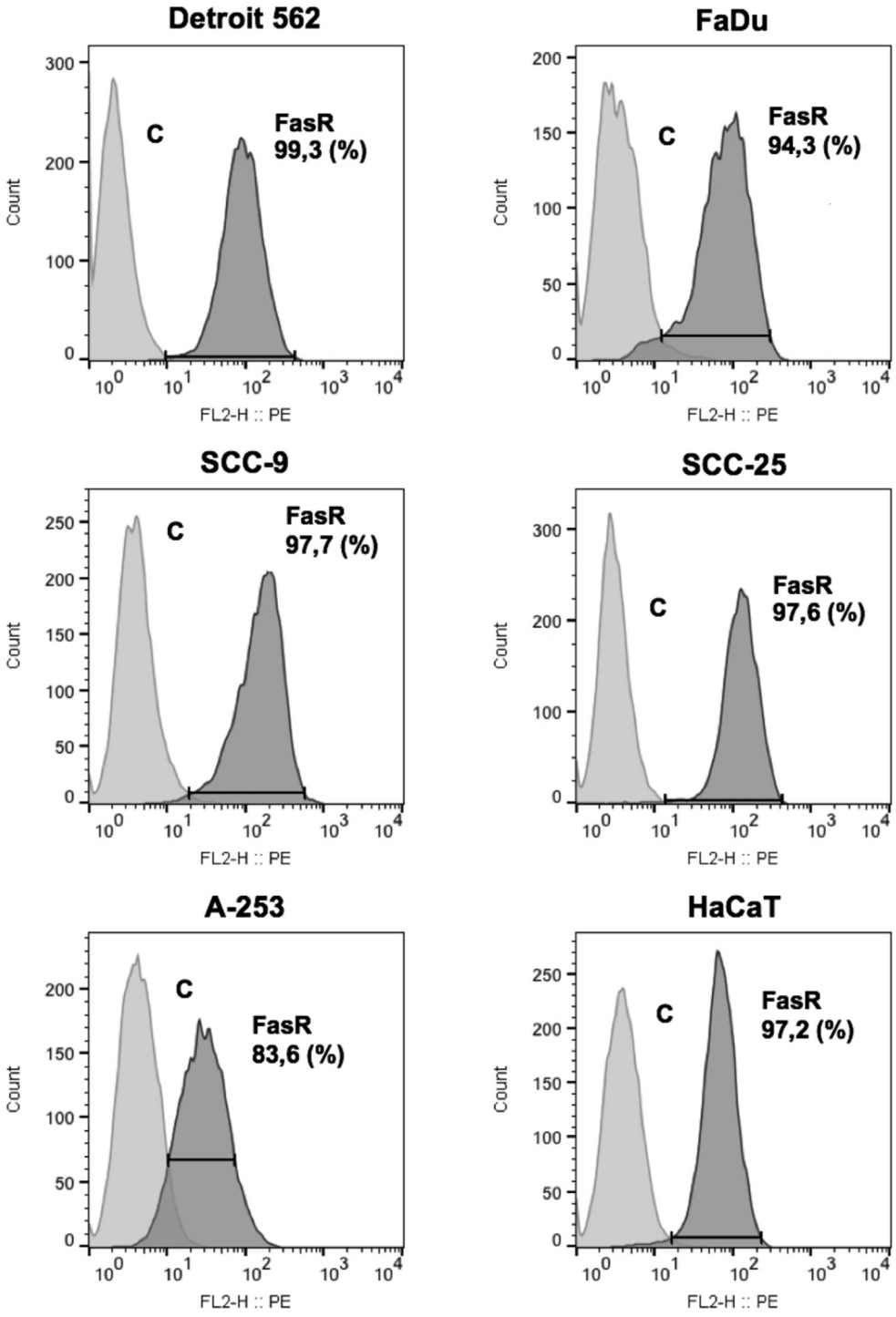

Fig. 1. FasR expression in OSCC cells. Flow cytometric analysis demonstrated distinct FasR expression across the cell panel. Expression is illustrated by a shift in the fluorescence peak on the x-axis (FL2-H: PE). Relative receptor expression (%) was detected by comparing FasR-expressing cells (dark gray peaks) to corresponding untreated control cells (light gray peaks).

($y < 1$) with significant sensitization ($p < 0.05$) in the dilution range from 3.13 to 25 ng/ml.

3.5. LCL161 induces apoptosis in OSCC cells

To detect apoptosis following exposure to LCL161, we performed Annexin V- and 7-AAD-based flow cytometry (Fig. 4). Incubation with LCL161 (IC_{100}; Table 2) caused distinct shifts in the cell population from Q4 (Annexin V−/7-AAD−: living cells) to Q2 (Annexin V+/7-AAD+: late apoptotic cells). LCL161 treatment also induced apoptosis in approximately 90% of the cells in all lines. Comparing apoptotic events at Q2 between the control and LCL161-treated samples, we detected very highly significant ($p < 0.001$) increases in apoptotic cells ranging from 2.1-fold (SCC-9) to 8.9-fold (A-253).

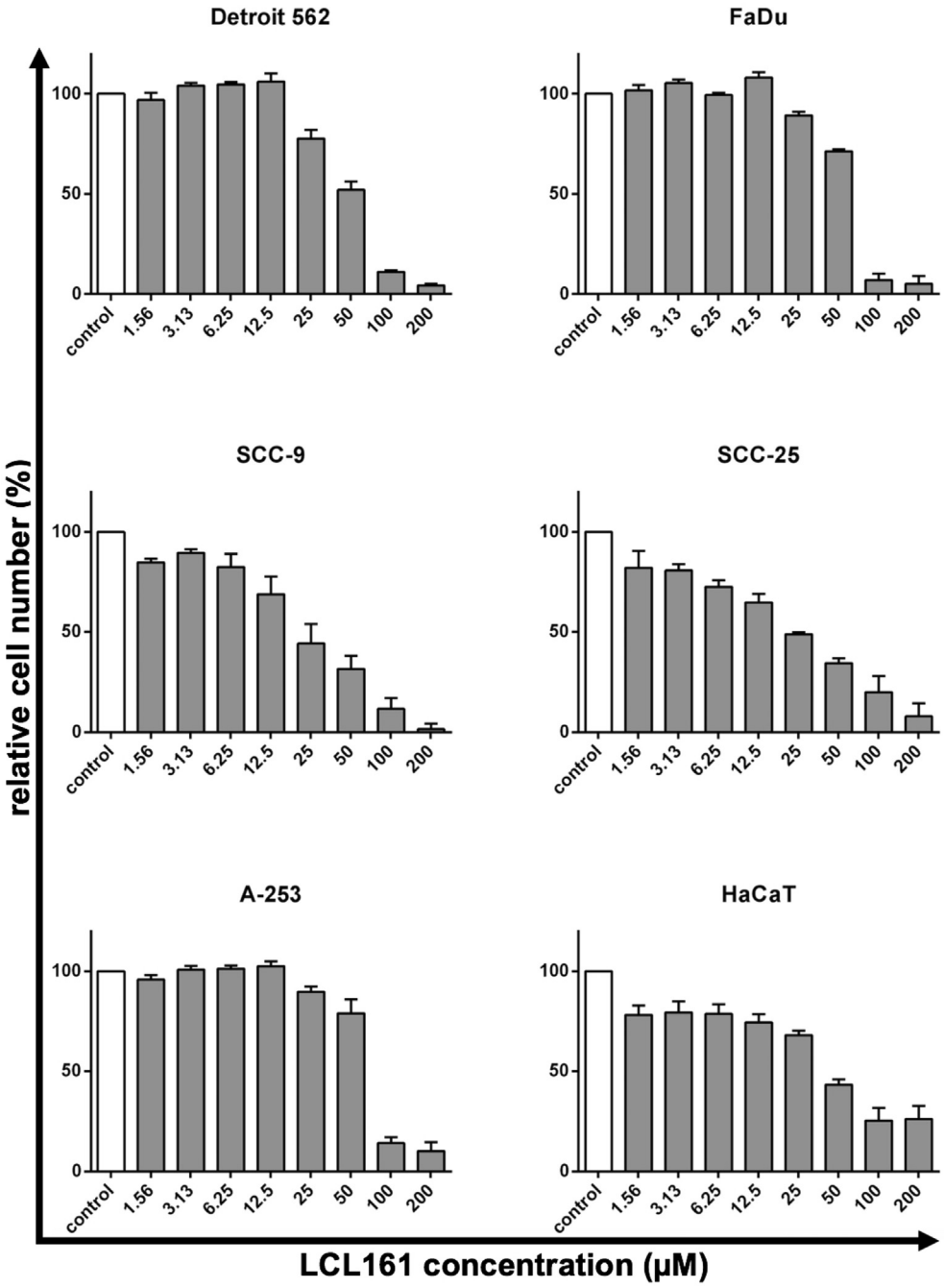

Fig. 2. LCL161 monotherapy in OSCC. The log2 dilutions of LCL161 starting at 200 µM are plotted on the x-axis. Relative cell number (%), measured by crystal violet assays after 72 h of incubation are plotted on the y-axis. White columns represent the control specimen treated with medium alone as a reference standard. As indicated by gray-shaded columns, LCL161 monotherapy demonstrated dose-dependent efficacy across the cell panel. The data correspond to the mean values of three independently executed assays ($n = 3$).

Proapoptotic effects of LCL161 were also illustrated by a shift in the peak corresponding to the FL2-H fluorescence channel (x-axis), representing Annexin V positivity, from fluorescence intensity level 10^1 for the control to 10^2 for LCL161-treated samples (data not shown).

3.6. Cell viability assay for the analysis of LCL161-induced programmed cell death

In general, apoptosis is activated by extrinsic and intrinsic pathways, both ending in the activation of effector caspases. Conversely, necroptosis is induced independently of caspases by receptor-interacting serine/threonine-protein kinase 1 (RIPK1). At the molecular level, both types of cell death are closely interlinked. While apoptosis is induced by activated caspase 8, necroptosis is suppressed by activated caspase 8 through RIPK1 inhibition (Pasparakis and Vandenabeele, 2015). In cancer cells, apoptosis is blocked by high levels of antiapoptotic proteins (e.g., IAPs) or inhibition of caspase 8 (Stupack, 2013). SMAC mimetics can contribute to the accumulation of RIPK1 via proteasomal degradation of cIAP^s (Petersen et al., 2010), and when apoptosis is

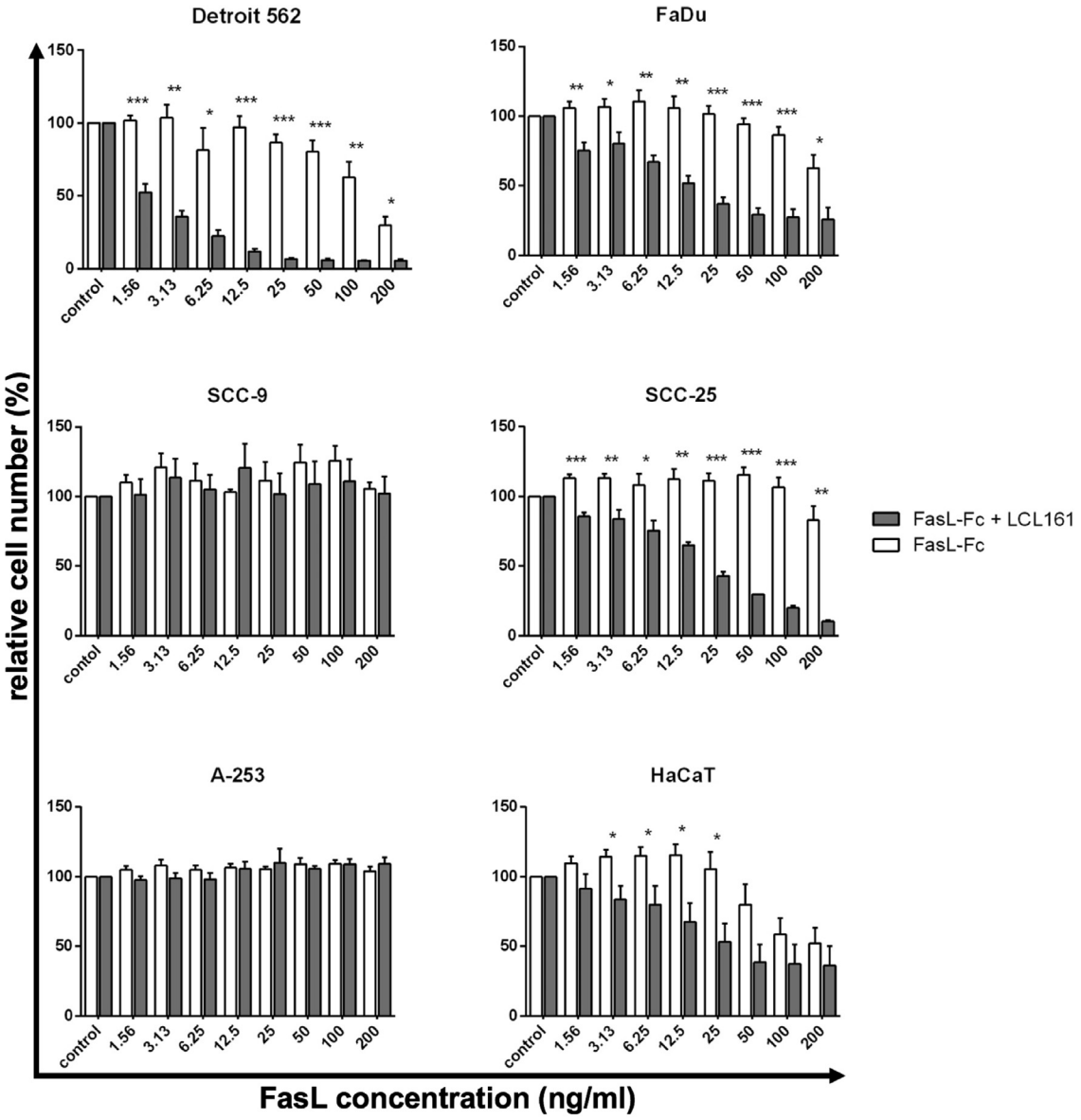

Fig. 3. FasL alone versus combination with LCL161. Results of crystal violet cytotoxicity assays comparing FasL alone and in combination with LCL161 (log_2 dilution starting at 200 ng/ml plus constant IC_{10} dose) for 72 h. To obtain mean values for statistical analysis, we performed three independent experiments ($n = 3$). White columns represent FasL alone; gray columns represent combination of FasL with LCL161. Statistical analysis: Significant values $p < 0.05$ comparing the corresponding dilution steps of FasL alone and in combination with LCL161 are indicated with *, highly significant $p < 0.01$ with ** and very highly significant $p < 0.001$ with ***.

suppressed, RIPK1 initiates necroptosis as a caspase-independent emergency program (Oberst, 2016). Thus, programmed cell death can be induced despite inhibition of apoptotic pathways. The pan-caspase inhibitor zVAD-fmk irreversibly suppresses caspase-mediated apoptosis, whereas Nec-1 acts as an RIPK1 inhibitor to block necroptosis. Due to crosstalk at FasR, simultaneous administration of both inhibitors is required (Pasparakis and Vandenabeele, 2015). In our study, the control cells proliferated even with a single application of zVAD-fmk and Nec-1, and administration of zVAD-fmk and Nec-1 (in combination) with LCL161 induced "rescue effects" in three of the six cell lines (SCC-9, SCC-25 and A-253) (Fig. 5) (Huang et al., 1862). Additionally, zVAD-fmk demonstrated generally stronger protective effects than did Nec-1, indicating that LCL161 caused caspase-mediated apoptotic cell death. Because the rescue effects were comparable with the cytoprotective effects in controls (zVAD-fmk, Nec-1 and zVAD-fmk + Nec-1), LCL161-induced cell death could not be prevented. Therefore, it can be assumed that the rescue effects were caused by general caspase inhibition, repressing the proapoptotic effects of LCL161. Interestingly, significant rescue effects were validated after adjusting for the growth effects of control cells only in FasL-resistant SCC-9 cells. Notably, neither apoptosis nor necroptosis was suppressed by the combination of zVAD-fmk and Nec-1.

4. Discussion

As the sixth most common malignancy, OSCC has considerable clinical and economic impact (Jou and Hess, 2017). However, since

Table 3
Quantitative and qualitative evaluations of the combination of LCL161 with FasL. List of FasL IC_{50} values for treatment alone and in combination (ng/ml). Tallarida's interaction index *y* for determining synergistic effects of the combination: * = synergistic effects, ** = additive effects, *** = antagonistic effects. For SCC-9 and A-253 cells, IC_{50} values could not be determined due to their resistance to FasL; therefore, the concentration of FasL was assumed to be 200 ng/ml.

Cell lines therapy	FasL IC_{50} (ng/ml)	Maximization of efficacy	Interaction index *y* (Tallarida)
Detroit 562:			
FasL	>51.1		
LCL161 [IC_{10}] + FasL	1.7	>30.1-fold	0.42*
FaDu			
FasL	>200		
LCL161 [IC_{10}] + FasL	5.2	>38.5-fold	0.44*
SCC-9			
FasL	/	/	
LCL161 [IC_{10}] + FasL	/	/	1.05***
SCC-25			
FasL	>200		
LCL161 [IC_{10}] + FasL	17	>11.8-fold	0.2*
A-253			
FasL	/	/	
LCL161 [IC_{10}] + FasL	/	/	1.37***
HaCaT			
FasL	51.2		
LCL161 [IC_{10}] + FasL	11	>4.7-fold	0.24*
Cumulative			
FasL	>125.6		
LCL161 [IC_{10}] + FasL	8.7	~15.6-fold	0.71*

the Food and Drug Administration (FDA) approved the anti-EGFR antibody cetuximab for adjuvant radiotherapy and palliative chemotherapy in head and neck cancer, no other medication has been approved, except for the monoclonal antibodies nivolumab and pembrolizumab (Larkins et al., 2017; Cetuximab approved by FDA, 2006; Ferris et al., 2016). One of the characteristics of OSCC is its ability to evade cell death. In addition to alterations and elevated levels of the tumor suppressor gene p53, overexpression of apoptosis inhibitors, including the proto-oncogene Bcl-2 and proinflammatory transcription factor NF-κB, is crucial in OSCC (Zhou et al., 2016; Wilson et al., 2001; Ondrey et al., 1999). More than 90% of all potentially malignant oral lesions overexpress IAPs (cIAP1, cIAP2, NAIP, XIAP, and Survivin) (Chen et al., 2011), and TCGA follow-up data for OSCC patients indicate alterations in IAP-encoding genes such as BIR-containing 2 (BIRC2), BIRC3, and XIAP in 12% of cases (Gao et al., 2013; Cerami et al., 2012). In addition, overexpression of this gene family results in poor prognosis with therapeutic resistance (Tanimoto et al., 2005; Yang et al., 2012). Patients who carry these mutations have a median survival of 29 months, whereas the survival rates are almost double in patients without these alterations (Gao et al., 2013; Cerami et al., 2012). Physiologically, SMAC is released from the mitochondria during intrinsic apoptosis as an IAP antagonist, which abolishes the inhibitory impact of IAPs on caspases. Therefore, the SMAC mimetic compound LCL161 is a potential agent for targeted therapy of OSCC. Various SMAC mimetics are currently in clinical trials for dose-escalation studies as monotherapy as well as combination therapy with chemotherapy and radiotherapy (Tolcher et al., 2016; Amaravadi et al., 2015; Infante et al., 2014).

4.1. LCL161 as a potential targeted therapeutic agent in selected OSCC cases

The SMAC mimetic compound LCL161 is a multi-IAP antagonist that induces proteasomal depletion of cIAP1 and cIAP2 and inhibition of XIAP (Wang et al., 2012; Falkenhorst et al., 2016). Alone, LCL161 exerted distinct cytotoxic effects across the OSCC cells examined. However, drug doses ranging from 100 to 200 μM were required to achieve adequate apoptotic effects. Moreover, induction of apoptotic cell death by LCL161 was confirmed by Annexin V FACS: for all six cell lines, approximately 90% of cells became apoptotic when stimulated with LCL161 at the IC_{100} concentration. Furthermore, the combination of LCL161 (at IC_{10}) and FasL significantly sensitized four of the six cell lines (Detroit 562, FaDu, SCC-25 and HaCaT) to FasL, representing synergistic effects. Interestingly, the initially nonresponsive cell line SCC-25 was highly significantly sensitized by LCL161 at minimal drug doses. In contrast, the other FasL-resistant cell lines SCC-9 and A-253 were not sensitized by this combination. Conceivably, the lack of IAP degradation in SCC-9 cells may be responsible for the observed treatment inefficacy (data not shown), as our group has already shown (Brands et al., 2016). Additional inhibitory proteins, e.g., survivin and cFLIP, may contribute to resistance in these cells (Khan et al., 2010; Li et al., 2008). In particular, constitutive NF-κB activation has been attributed to the lack of response of SCC-9 cells to TNF-α (Duffey et al., 2000). In contrast, HaCaT cells are potently sensitized by LCL161 at low doses (IC_{10} of 0.6 μM), emphasizing the general high potency of this agent. Interestingly, no degrading effects of LCL161 were detectable at the protein level (data not shown), indicating that in addition to the degrading effects on IAPs, LCL161 might exert inhibitory effects sufficient for apoptotic sensitization. Nonetheless, the concentrations of LCL161 required for *in vitro* treatment may limit its clinical application. Yang et al. (2015) published IC_{50} doses ranging from 32 to 95 μM for OSCC *in vitro* treatment, which are fully in accordance with our data. However, because of a cytokine release syndrome (CRS) as a limiting event induced by LCL161-mediated NF-κB activation, Infante et al. (2014) reported a maximum tolerated dose (MTD) of 1,800 mg in their dose escalation study, though the authors did not provide any evidence of efficacy for LCL161 alone. A plausible application of this agent might be in an adjuvant manner as combinational therapy as part of personalized medicine in selected

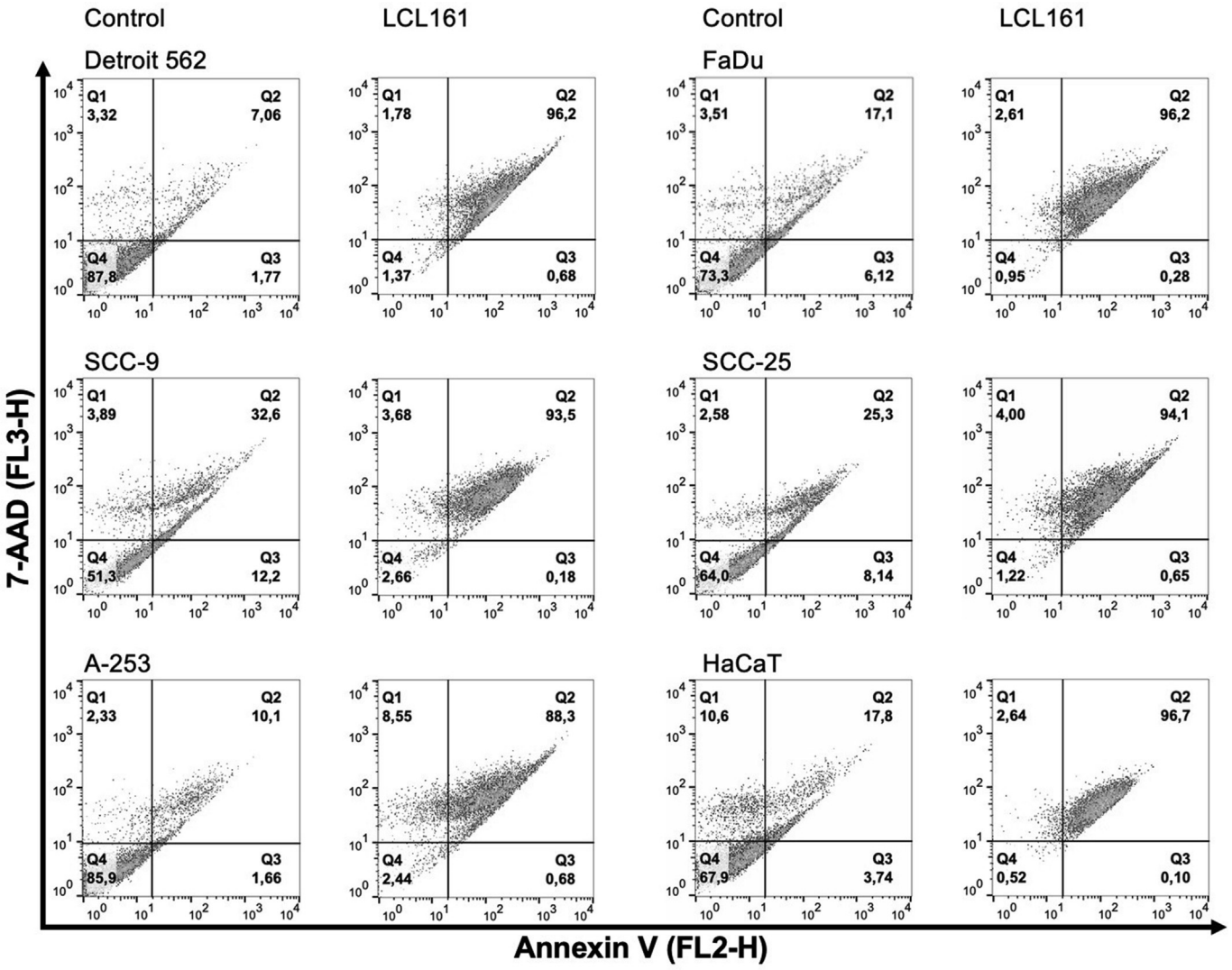

Fig. 4. Annexin V and 7-AAD FACS apoptosis assay. OSCC Detroit 562, FaDu, SCC-9 and SCC-25 cells (reference cells: A-253 and HaCaT) were pretreated with LCL161 (IC_{100}) for 48 h. Dot plots are separated into 4 quadrants: Q1 (Annexin V−/7-AAD+: nonspecific cell death), Q2 (Annexin V+/7-AAD+: late apoptotic cells), Q3 (Annexin V+/7-AAD−: early apoptotic cells) and Q4 (Annexin V−/7-AAD−: living cells). Distinct shifts in fluorescence intensity were observed in all LCL161-stimulated cell lines ($n = 3$).

patients. Similar to our study, others have reported apoptosis-sensitizing effects of LCL161 in combination with radiotherapy in OSCC, effects that were attributed to increased caspase activation, supporting the potent proapoptotic impact of LCL161 as a part of IAP-targeting therapy regimens (Yang et al., 2016; Brands et al., 2016; Qin et al., 2014).

4.2. LCL161-induced apoptosis cannot be prevented

Although cell viability assays did not clearly differentiate the type of programmed cell death triggered by LCL161, in connection with FACS analysis, we conclude that LCL161 induces apoptosis in the cells used in this study. Apoptotic signaling mediated by complex IIa can be blocked in OSCC cells. Under conditions of IAP overexpression and caspase suppression, proinflammatory pathways mediated by complex I are considered to lead to resistance, cell survival and proliferation via the NF-κB signaling pathway and MAPK cascades, explaining the increase in cell number in response to zVAD-fmk (Seger and Krebs, 1995). Thus, degradation of IAPs might create an avalanche-like, proapoptotic milieu in OSCC cells, which, once activated, cannot be stopped. By activating the E3-ubiquitin ligase activity of IAPs, SMAC mimetics induce autoubiquitination and subsequent proteasomal degradation of cIAPs, rendering apoptosis induction irreversible (Varfolomeev et al., 2007; Wu et al., 2007). Therefore, FasL may initiate apoptosis via complex IIa in OSCC cells.

5. Conclusion

In conclusion, combination therapies with proapoptotic sensitization effects have emerged as a potential treatment option for cancer. The approach of this targeted inhibition of apoptosis might be suitable for the individualized therapy of OSCC. The combination of LCL161 with cell cycle inhibitors, immune checkpoint inhibitors, etc. could be promising in terms of clinical translation, since a synergistic and non-competitive effect can be assumed, as this study demonstrates through the use of receptor antibodies. Nevertheless, further studies are needed to elucidate the molecular mechanisms and interactions leading to treatment failure and help overcome these mechanisms by IAP-targeting therapy.

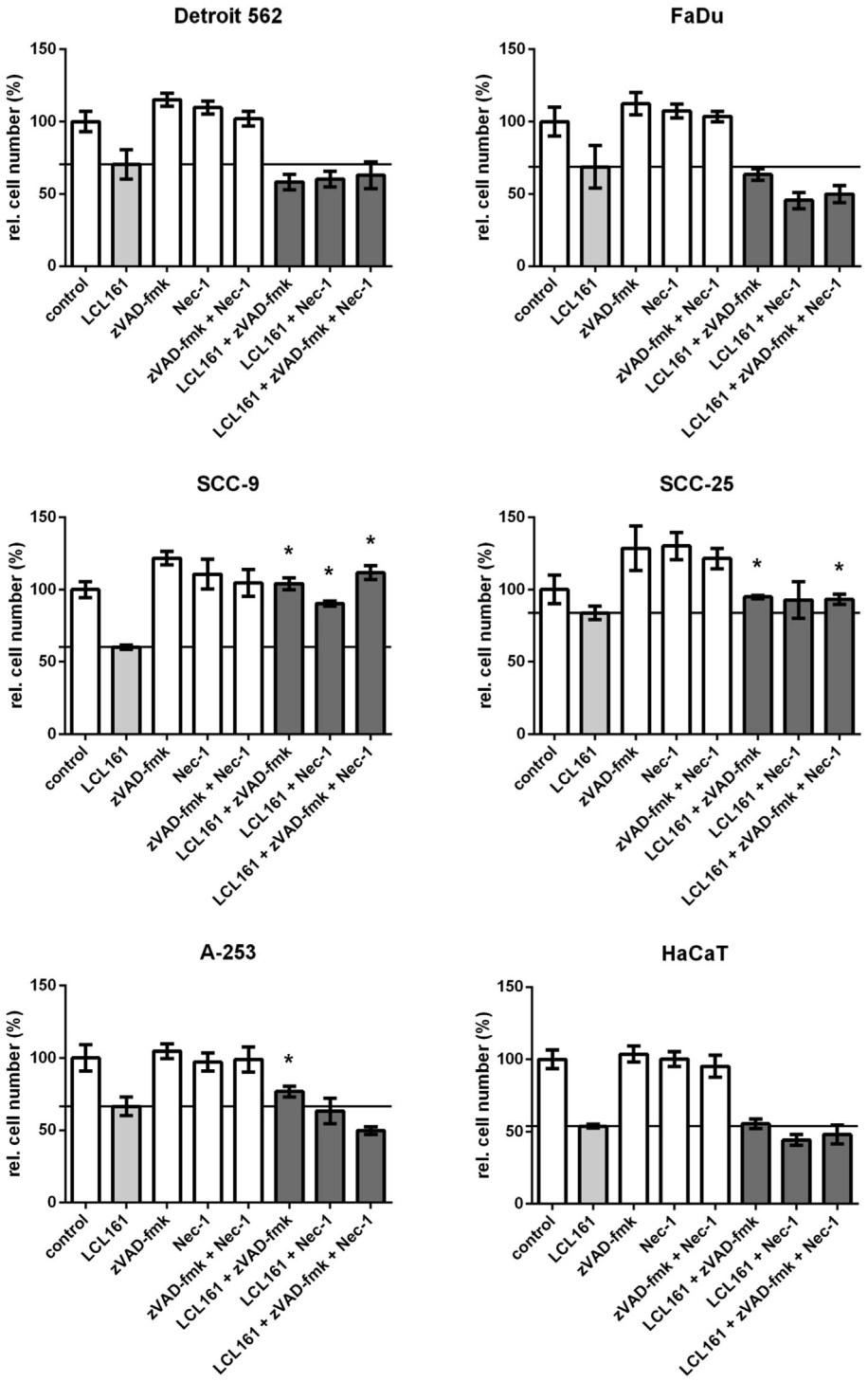

Fig. 5. Cell viability assay to detect the type of programmed cell death induced by LCL161 in OSCC. Cells were incubated with LCL161 (IC_{90}), zVAD-fmk (50 μM), Nec-1 (90 μM) or the combination of all agents (LCL161 + zVAD-fmk/Nec-1/[zVAD-fmk + Nec-1]) for 24 h. Quantification was carried out with crystal violet assays. Distinct "rescue effects" were observed in three of the six cell lines (SCC-9, SCC-25 and A-253). The significantly higher increase in relative cell count in zVAD-fmk and/or Nec-1 (co)-treated samples compared with LCL161-treated samples was defined as the "rescue effect", as marked with asterisks. The results were considered significant if there was no overlap in the error bar between LCL161 alone and the LCL161 + zVAD/Nec-1/[zVAD-fmk + Nec-1] combination. The results indicate that LCL161-induced programmed cell death is mediated by caspases in OSCC and is therefore apoptotic.

Funding

The present study was supported by the Comprehensive Cancer Center Mainfranken (CCC MF) and the Interdisciplinary Center for Clinical Research (IZKF), Würzburg, Germany.

Availability of data and materials

The datasets used and/or analyzed during the current study are available from the corresponding author on reasonable request.

Ethics approval and consent to participate

This article does not contain any studies with human participants or animals performed by any of the authors.

Patient consent for publication

For this type of study, patient consent is not required.

Conflicts of interest

The authors declare that there are no conflicts of interest with any financial organizations regarding the material discussed in this manuscript.

Appendix A. Supplementary data

Supplementary data to this article can be found online at https://doi.org/10.1016/j.jcms.2019.07.022.

References

Amaravadi RK, Schilder RJ, Martin LP, Levin M, Graham MA, Weng DE, Adjei AA: A Phase I study of the SMAC-mimetic birinapant in adults with refractory solid tumors or lymphoma. Mol Cancer Ther 14: 2569–2575, 2015

Bai L, Smith DC, Wang S: Small-molecule SMAC mimetics as new cancer therapeutics. Pharmacol Ther 144: 82–95, 2014

Brands RC, Herbst F, Hartmann S, Seher A, Linz C, Kubler AC, Muller-Richter UDA: Cytotoxic effects of SMAC-mimetic compound LCL161 in head and neck cancer cell lines. Clin Oral Investig 20: 2325–2332, 2016

Brands RC, Scheurer MJJ, Hartmann S, Seher A, Kübler AC, Müller-Richter UDA: Apoptosis-sensitizing activity of birinapant in head and neck squamous cell carcinoma cell lines. Oncol Lett 15: 4010–4016, 2018

Cerami E, Gao J, Dogrusoz U, Gross BE, Sumer SO, Aksoy BA, Jacobsen A, Byrne CJ, Heuer ML, Larsson E, et al: The cBio cancer genomics portal: an open platform for exploring multidimensional cancer genomics data. Cancer Discov 2: 401–404, 2012

Cetuximab approved by FDA for treatment of head and neck squamous cell cancer. Cancer Biol Ther 5: 340–342, 2006

Chapman CH, Saba NF, Yom SS: Targeting epidermal growth factor receptor for head and neck squamous cell carcinoma: still lost in translation? Ann Transl Med 4: 80, 2016

Chen YK, Huse SS, Lin LM: Expression of inhibitor of apoptosis family proteins in human oral squamous cell carcinogenesis. Head Neck 33: 985–998, 2011

Crook NE, Clem RJ, Miller LK: An apoptosis-inhibiting baculovirus gene with a zinc finger-like motif. J Virol 67: 2168–2174, 1993

Deveraux QL, Reed JC: IAP family proteins—suppressors of apoptosis. Genes Dev 13: 239–252, 1999

Döbrossy L: Epidemiology of head and neck cancer: magnitude of the problem. Cancer Metastasis Rev 24: 9–17, 2005

Du C, Fang M, Li Y, Li L, Wang X: SMAC, a mitochondrial protein that promotes cytochrome c-dependent caspase activation by eliminating IAP inhibition. Cell 102: 33–42, 2000

Duffey DC, Crowl-Bancroft CV, Chen Z, Ondrey FG, Nejad-Sattari M, Dong G, Van Waes C: Inhibition of transcription factor nuclear factor-kappaB by a mutant inhibitor-kappaBalpha attenuates resistance of human head and neck squamous cell carcinoma to TNF-alpha caspase-mediated cell death. Br J Cancer 83: 1367–1374, 2000

Elmore S: Apoptosis: a review of programmed cell death. Toxicol Pathol 35: 495–516, 2007

Falkenhorst J, Grunewald S, Muhlenberg T, Marino-Enriquez A, Reis AC, Corless C, Heinrich M, Treckmann J, Podleska LE, Schuler M, et al: Inhibitor of Apoptosis Proteins (IAPs) are commonly dysregulated in GIST and can be pharmacologically targeted to enhance the pro-apoptotic activity of imatinib. Oncotarget 7: 41390–41403, 2016

Ferris RL, Blumenschein G, Fayette J, Guigay J, Colevas AD, Licitra L, Harrington K, Kasper S, Vokes EE, Even C, et al: Nivolumab for recurrent squamous-cell carcinoma of the head and neck. N Engl J Med 375: 1856–1867, 2016

Fulda S: SMAC mimetics as IAP antagonists. Semin Cell Dev Biol 39: 132–138, 2015

Gao J, Aksoy BA, Dogrusoz U, Dresdner G, Gross B, Sumer SO, Sun Y, Jacobsen A, Sinha R, Larsson E, et al: Integrative analysis of complex cancer genomics and clinical profiles using the cBioPortal. Sci Signal 6: pl1, 2013

Grandis JR, Tweardy DJ: Elevated levels of transforming growth factor alpha and epidermal growth factor receptor messenger RNA are early markers of carcinogenesis in head and neck cancer. Cancer Res 53: 3579–3584, 1993

Gupta S, Kong W, Peng Y, Miao Q, Mackillop WJ: Temporal trends in the incidence and survival of cancers of the upper aerodigestive tract in Ontario and the United States. Int J Cancer 125: 2159–2165, 2009

Gyrd-Hansen M, Meier P: IAPs: from caspase inhibitors to modulators of NF-kappaB, inflammation and cancer. Nat Rev Cancer 10: 561–574, 2010

Hanahan D, Weinberg RA: Hallmarks of cancer: the next generation. Cell 144: 646–674, 2011

Huang Z, Epperly M, Watkins SC, Greenberger JS, Kagan VE, Bayir H: Necrostatin-1 rescues mice from lethal irradiation. Biochim Biophys Acta 1862: 850–856, 2016

Infante JR, Dees EC, Olszanski AJ, Dhuria SV, Sen S, Cameron S, Cohen RB: Phase I dose-escalation study of LCL161, an oral inhibitor of apoptosis proteins inhibitor, in patients with advanced solid tumors. J Clin Oncol 32: 3103–3110, 2014

Jou A, Hess J: Epidemiology and molecular biology of head and neck cancer. Oncol Res Treat 40: 328–332, 2017

Khan Z, Khan N, Tiwari RP, Patro IK, Prasad GB, Bisen PS: Down-regulation of survivin by oxaliplatin diminishes radioresistance of head and neck squamous carcinoma cells. Radiother Oncol 96: 267–273, 2010

LaCasse EC, Mahoney DJ, Cheung HH, Plenchette S, Baird S, Korneluk RG: IAP-targeted therapies for cancer. Oncogene 27: 6252–6275, 2008

Lagler C, El-Mesery M, Kübler AC, Müller-Richter UDA, Stühmer T, Nickel J, Müller TD, Wajant H, Seher A: The anti-myeloma activity of bone morphogenetic protein 2 predominantly relies on the induction of growth arrest and is apoptosis-independent. PLoS One 12: e0185720, 2017

Larkins E, Blumenthal GM, Yuan W, He K, Sridhara R, Subramaniam S, Zhao H, Liu C, Yu J, Goldberg KB, et al: FDA Approval summary: pembrolizumab for the treatment of recurrent or metastatic head and neck squamous cell carcinoma with disease progression on or after platinum-containing chemotherapy. Oncologist 22: 873–878, 2017

Li X, Pan X, Zhang H, Lei D, Liu D, Xu F, Luan X: Overexpression of cFLIP in head and neck squamous cell carcinoma and its clinicopathologic correlations. J Cancer Res Clin Oncol 134: 609–615, 2008

Matta A, Ralhan R: Overview of current and future biologically based targeted therapies in head and neck squamous cell carcinoma. Head Neck Oncol 1: 6, 2009

Nagata M, Nakayama H, Tanaka T, Yoshida R, Yoshitake Y, Fukuma D, Kawahara K, Nakagawa Y, Ota K, Hiraki A, et al: Overexpression of cIAP2 contributes to 5-FU resistance and a poor prognosis in oral squamous cell carcinoma. Br J Cancer 105: 1322–1330, 2011

Nikoletopoulou V, Markaki M, Palikaras K, Tavernarakis N: Crosstalk between apoptosis, necrosis and autophagy. Biochim Biophys Acta 1833: 3448–3459, 2013

Oberst A: Death in the fast lane: what's next for necroptosis? FEBS J 283: 2616–2625, 2016

Ondrey FG, Dong G, Sunwoo J, Chen Z, Wolf JS, Crowl-Bancroft CV, Mukaida N, van Waes C: Constitutive activation of transcription factors NF-(kappa)B, AP-1, and NF-IL6 in human head and neck squamous cell carcinoma cell lines that express pro-inflammatory and pro-angiogenic cytokines. Mol Carcinog 26: 119–129, 1999

Pasparakis M, Vandenabeele P: Necroptosis and its role in inflammation. Nature 517: 311–320, 2015

Petersen SL, Peyton M, Minna JD, Wang X: Overcoming cancer cell resistance to SMAC mimetic induced apoptosis by modulating cIAP-2 expression. Proc Natl Acad Sci U S A 107: 11936–11941, 2010

Qi S, Mogi S, Tsuda H, Tanaka Y, Kozaki K, Imoto I, Inazawa J, Hasegawa S, Omura K: Expression of cIAP-1 correlates with nodal metastasis in squamous cell carcinoma of the tongue. Int J Oral Maxillofac Surg 37: 1047–1053, 2008

Qin Q, Zuo Y, Yang X, Lu J, Zhan L, Xu L, Zhang C, Zhu H, Liu J, Liu Z, et al: SMAC mimetic compound LCL161 sensitizes esophageal carcinoma cells to radiotherapy by inhibiting the expression of inhibitor of apoptosis protein. Tumour Biol 35: 2565–2574, 2014

Ramakrishnan V, Painuly U, Kimlinger T, Haug J, Rajkumar SV, Kumar S: Inhibitor of apoptosis proteins as therapeutic targets in multiple myeloma. Leukemia 28: 1519–1528, 2014

Ribas A: Tumor immunotherapy directed at PD-1. N Engl J Med 366: 2517–2519, 2012

Seger R, Krebs EG: The MAPK signaling cascade. FASEB J 9: 726–735, 1995

Stupack DG: Caspase-8 as a therapeutic target in cancer. Cancer Lett 332: 133–140, 2013

Tallarida RJ: The interaction index: a measure of drug synergism. Pain 98: 163–168, 2002

Tamatani T, Takamaru N, Uchida D, Nagai H, Fujisawa K, Miyamoto Y: The expression of X-linked inhibitor of apoptosis in human oral squamous cell carcinoma and its relationship with clinical factors. Cancer Res 72: 4954, 2012

Tanimoto T, Tsuda H, Imazeki N, Ohno Y, Imoto I, Inazawa J, Matsubara O: Nuclear expression of cIAP-1, an apoptosis inhibiting protein, predicts lymph node metastasis and poor patient prognosis in head and neck squamous cell carcinomas. Cancer Lett 224: 141–151, 2005

Tolcher AW, Bendell JC, Papadopoulos KP, Burris HA, Patnaik A, Fairbrother WJ, Wong H, Budha N, Darbonne WC, Peale F, et al: A Phase I dose-escalation study evaluating the safety tolerability and pharmacokinetics of CUDC-427, a potent, oral, monovalent iap antagonist, in patients with refractory solid tumors. Clin Cancer Res 22: 4567–4573, 2016

Varfolomeev E, Blankenship JW, Wayson SM, Fedorova AV, Kayagaki N, Garg P, Zobel K, Dynek JN, Elliott LO, Wallweber HJ, et al: IAP antagonists induce autoubiquitination of c-IAPs, NF-kappaB activation, and TNFalpha-dependent apoptosis. Cell 131: 669–681, 2007

Vigneswaran N, Williams MD: Epidemiologic trends in head and neck cancer and aids in diagnosis. Oral Maxillofac Surg Clin North Am 26: 123–141, 2014

Wang S, Bai L, Lu J, Liu L, Yang CY, Sun H: Targeting Inhibitors of Apoptosis Proteins (IAPs) for new breast cancer therapeutics. J Mammary Gland Biol Neoplasia 17: 217–228, 2012

Wilson GD, Saunders MI, Dische S, Richman PI, Daley FM, Bentzen SM: Bcl-2 expression in head and neck cancer: an enigmatic prognostic marker. Int J Radiat Oncol Biol Phys 49: 435–441, 2001

Wu H, Tschopp J, Lin SC: SMAC mimetics and TNFalpha: a dangerous liaison? Cell 131: 655–658, 2007

Yang XH, Feng ZE, Yan M, Hanada S, Zuo H, Yang CZ, Han ZG, Guo W, Chen WT, Zhang P: XIAP is a predictor of cisplatin-based chemotherapy response and prognosis for patients with advanced head and neck cancer. PLoS One 7: e31601, 2012

Yang L, Kumar B, Romito M, Teknosa TN, Chakravarti A, Williams TM: Abstract C144: LCL161, a SMAC mimetic, induces preferential radiosensitization in human papillomavirus negative head and neck squamous cell carcinoma through induction of apoptosis. Mol Cancer Ther 14: C144, 2015

Yang C, Wang H, Zhang B, Chen Y, Zhang Y, Sun X, Xiao G, Nan K, Ren H, Qin S: LCL161 increases paclitaxel-induced apoptosis by degrading cIAP1 and cIAP2 in NSCLC. J Exp Clin Cancer Res 35: 158, 2016

Zhou G, Liu Z, Myers JN: TP53 Mutations in head and neck squamous cell carcinoma and their impact on disease progression and treatment response. J Cell Biochem 117: 2682–2692, 2016